Eur. Phys. J. B **52**, 41–46 (2006)
DOI: 10.1140/epjb/e2006-00272-0

THE EUROPEAN PHYSICAL JOURNAL B

Optical properties of ZnO related to the dc sputtering power

A. Ahmad[a] and A. Alsaad

Department of Physical Sciences, Jordan University of Science & Technology, P.O. Box 3030, Irbid-22110, Jordan

Received 13 March 2006 / Received in final form 14 June 2006
Published online 6 July 2006 –

Abstract. Zinc oxide thin films were sputter deposited on (100) silicon substrates at 250 °C substrates temperature via reactive unbalanced dc magnetron process using pure zinc target and argon/oxygen gases. The influence of the applied dc sputtering power (between 100 to 250 Watts, step 50 Watts) on the optical properties of the grown films was systematically investigated by variable angle of incidence spectroscopic ellipsometry (VASE) technique. The refractive indices were found to follow the second-order Sellmeier dispersion relation. However, Cauchy-like dispersion model was formulated to account for the absorption tail and excitonic structure near the direct band gap. The optical properties such as refractive indices, extinction coefficients, optical band gaps, Urbach's energies, excitonic binding structure and absorption coefficients of the grown films were reported as a function of dc power in the photon energy range between 1.2 eV and 4.2 eV. The films were found to be polycrystalline with (002) preferred orientation.

PACS. 78.20.Ci Optical constants (including refractive index, complex dielectric constant, absorption, reflection and transmission coefficients, emissivity) – 81.15.Cd Deposition by sputtering – 81.40.Tv Optical and dielectric properties (related to treatment conditions)

1 Introduction

Zinc oxide (ZnO) is an n-type, wide direct band gap semiconductor of around 3.4 eV with high exciton binding energy (60 meV) even at room temperature [1,2]. This thin film has attracted much attention because of its potential in many applications such as optoelectronic devices, solar cells, optical coatings and surface acoustic wave devices. Like most of Nitride semiconductors, such as GaN, InN and AlN, the ZnO adopts the four-times coordinated wurtzite phase in its ground state that belongs to the hexagonal h_c symmetry group and thus plays an important role in many fundamental and technological applications [3]. Based on the fact that oxygen plays an important role in the conduction mechanism of the ZnO material due to their interstitial, oxygen vacancy V_{O} or anti site defect with zinc atoms $\mathrm{O_{Zn}}$, the films stoichiometry become very good candidates for $\mathrm{O_2}$ gas sensors [4–7]. It is well-known that ZnO optical and physical properties depend on the method of preparation. Several techniques have been implemented in the preparation of these important technological thin films such as pulsed laser deposition [8], chemical vapor deposition (CVD) [9], pyrolytic deposition [10], sol-gel process [11], dc [12–14] and rf sputter deposition [15,16].

Usually zinc oxide ceramic targets are used to sputter-deposit films of similar stoichiometry. The rf plasma discharges are used for such sputtering technique to avoid target-surface charge accumulation and hence, target heating and loss of sputtering yield. For the best of our knowledge, few experimental studies have been carried out on depositing ZnO films from metallic zinc targets and reactive gases such as oxygen [8,9,16]. In the current work, however, a 99.99% pure metallic zinc target along with argon/oxygen gas mixture is used to deposit ZnO thin films on Si(100) substrates via reactive unbalanced magnetron dc sputtering process. The optical properties including Urbach's energies and band gaps of the films obtained by variable angle of incidence spectroscopic ellipsometry (VASE) technique are evaluated as a function of the applied dc power accordingly [12,13,17].

2 Experiment

2.1 Film preparation

The reactive unbalanced magnetron sputter deposition of the ZnO films was performed in a commercial cryo-pumped stainless steel chamber with a base pressure of less than or equal to 10^{-6} Torr. The flow rate and partial pressure of argon/oxygen were maintained at 7.5/15 $\mathrm{cm^3/s}$. and 6.6/1.4 mTorr, respectively. A small drop of silver paint was placed and dried on the surface of the silicon substrate before it is mounted 8 cm away from the zinc target-surface in the chamber. The silicon substrate was placed on an electrically floating sample-holder mounted on a heater-plate heated to 250 °C. The sputter gun was

[a] e-mail: sema@just.edu.jo; sema_just@yahoo.com

operated by a dc power supply maintained at constant value of 100, 150, 200 or 250 Watts in each deposition run. A pre-sputtering process with argon gas was performed for thirty minutes in order to stabilize the glow discharge and clean the target surface before the film deposition takes place. The silver paint is easily pealed off the sample surface after the film deposition leaving step-up profile between the film and substrate surfaces. The film thickness was then measured by a step-up mechanical stylus machine. The deposition rate for each film is calculated using the film thickness obtained by the mechanical stylus divided by the real time of deposition.

2.2 Spectroscopic ellipsometry

A non-destructive ellipsometric measurements were performed in an ex situ mode on all the samples using variable angle spectroscopic ellipsometry (VASE, J. A. Woollam Co., Inc., Lincoln, NE) [18]. Spectroscopic scans over three angles of incidence ($\phi = 60°$, 65° and 70° were used over a wavelength range between 300 and 1000 nm (≈1.2 and 4.2 eV) to solve independently for the film thickness and the unique optical constants. The ellipsometric parameters ψ and Δ were measured by the automated rotating analyzer ellipsometer in steps of 2 nm of wavelengths. Each ψ or Δ value is averaged over thirty measured values. The measured quantities were expressed in terms of a complex number ρ that is a function of ordinary and extraordinary waves containing the ellipsometric values ψ and Δ as [19]:

$$\rho = \frac{R_p}{R_s} = \tan\psi e^{i\Delta} = \mathrm{Re}(\rho) + i\mathrm{Im}(\rho)$$
$$= \tan\psi\cos\Delta + i\tan\psi\sin\Delta, \quad (1)$$

where, R_p and R_s are the complex reflection coefficients for the light polarized parallel (p) and perpendicular (s) to the plane of incidence, respectively. Since ZnO crystals are known to be an-isotropic, the ellipsometric measurements are unable to separate the two components of the dielectric function of this configuration. Hence, the wave propagation directions in the ZnO layer changes only insignificantly under the mode-setting of our experimental ellipsometric acquisition mode and therefore, the resultant dielectric function and equivalently, the refractive index is a mixture of both $\varepsilon_\perp$ and $\varepsilon_{//}$ (ordinary $n_\perp$ and extraordinary $n_{//}$) [20]. All measurements were performed in the ex situ mode at room temperatures. The measured ψ and Δ curves are converted into optical constants such as the real and imaginary parts of the complex refractive index in the form of $\varepsilon = (n + ik)^2$ and the real and imaginary parts of the complex dielectric function ($\varepsilon = \varepsilon_1 + i\varepsilon_2$). The angles ($\psi$ and Δ) are related to each other by Kramers-Kronig dispersion relations that are essential for many-parameter determination from measured data [19–21]. Figures 1 and 2 show sample of the measured and generated ψ and Δ spectra, respectively for a film deposited at 100 Watt power. The fittings are based on the parametric modified model dielectric function which will be disused in Section 3.1.

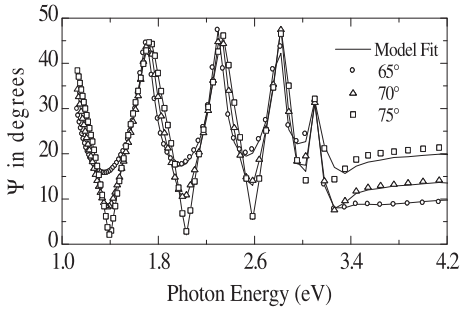

Fig. 1. Experimental and generated spectra for ψ given at three incident angles.

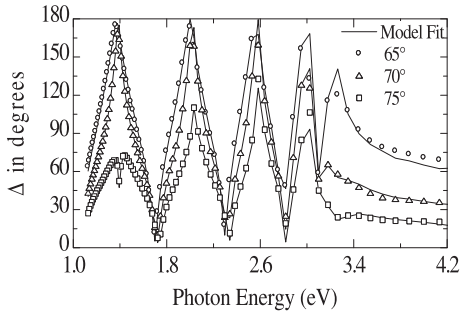

Fig. 2. Experimental and generated spectra for Δ given at three incident angles.

The fluctuations in ψ and Δ curves, plotted as a function of incident energy or wavelength, are due to the interference in the film-thickness which is found to be around 450 nm.

3 Results and discussion

3.1 Model dielectric function for ZnO

Spectroscopic ellipsometry measurements were performed for ZnO films by many researchers. Jellison and Boatner [22] have used a two-modular generalized ellipsometer for appropriate aligned uniaxial ZnO crystals to find almost accurate values of optical functions above the direct band gap. However, the optical constants near the band edge were fitted to a modified model dielectric function (MDF) developed by Holden et al. [23] based on the electronic energy-band structure with excitonic interaction of three-dimensional critical point. Yoshikawa and Adachi [24] have improved a theoretical model for the dielectric function for single crystalline ZnO based on the direct interband transition from the highest valence band to the lowest conduction band considering the conduction band as s-like having Γ symmetry while the valence band as a p-like, splitting into three doubly degenerate band due to split orbit and crystal field interactions. The automatic ellipsometer used in their experimental part was able to carry out the ellipsometric measurements on the

Table 1. Experimental and fitted results obtained for the ZnO samples.

dc power (Watts)	Thickness in (nm) by: Stylus	Ellipsometer	EMA roughness (nm)	Void % in EMA layer	Sputter rate nm/s
100	450	421	68.5	78.72	0.25
150	540	518	68.6	77.05	0.45
200	690	660	66.5	73.50	0.49
250	400	430	42.8	68.70	0.42

surface parallel to the optic c-axis, which allowed the determination of the optical constants for polarization perpendicular and parallel to the c-axis. Based on this model, Yoshikawa and Adachi [24] have used the first-order Sellmeier equation for the refractive index in the region below and near the fundamental absorption edge. They found their results to agree with similar optical functions obtained by both Bond [25] and Mollwo and Swinney [26] via prism method. Later, Sun and Kowk [1] have used the second-order Sellmeier equation for the refractive index n, and zero extinction coefficient k, based on the fact that ZnO absorbs very little in the near UV and visible region. In a second step of analysis, they extended the regression fit for k into the UV region and found their results to agree with those in the literature [27]. A layer model-based regression analysis using an error function weighted to the experimental error was performed by Rebien et al. [28] to extract the optical constants as well as the film thickness and surface roughness from spectral point by point fit [29]. Teng et al. [30] have used the first-order Sellmeier dispersion relation for a model dielectric function to evaluate the refractive index of MgZnO. They modeled the excitonic absorption of a single ZnO crystal by discrete states of excitons with a broadened Lorentzian line shape [31]. Postava et al. [26] have improved the model dielectric function by including Lorentz approximation of line broadening and high-energy absorption term to account for Kramers-Kronig relations. Accordingly, a first-order Sellmeier form function was used for epitaxial ZnO formulation.

Although the ZnO films deposited in our technique have shown a preferred (002) orientation, however, still there are other weak polycrystalline orientations seen in the films such as ZnO(101) and ZnO(100) as well as Zn(101) material. Based on the fact that in dealing with polycrystalline material, a second-order wavelength-dependent Sellmeier's refractive index dispersion formula has been used to account for the model dielectric function in the form [26]:

$$n(\lambda)^2 = A_n + \frac{B_n\lambda^2}{\lambda^2 - C_n^2} + \frac{D_n\lambda^2}{\lambda^2 - E_n^2}, \qquad (2)$$

where, A_n, B_n, C_n, D_n and E_n are the fitting parameters. The steepness and band tailing (Urbach's energy) in the exponential transition decay below the band edge as well as the excitonic structure below and near the direct band gap are formulated by Cauchy-like dispersion expression as [23,24,30,32]:

$$k(\lambda) = F_k\lambda e^{-G_k\left(\frac{1}{H_k}-\frac{1}{\lambda}\right)}, \qquad (3)$$

where, F_k, G_k, and H_k are also fitting parameters.

A regression analysis was performed to calculate ψ and Δ based on a model dielectric function (MDF) for the structure using Fresnel's equations for reflection of polarized light from planar media. While analyzing the samples, the silicon substrate optical constants were used from the tabulated results in the literature [33]. The film thickness obtained from the mechanical stylus was used as a starting raw value in the ellipsometric analyses technique. However, Cauchy-like and Sellmeier's model-parameters were systematically allowed to vary until the generated ψ and Δ curves have best fitted the measured curves. In all the cases, the parameters correlation matrix and 90% fitting confidence limit were confirmed for non-problematic causes. The film thickness was then added to the fitting parameters to be solved for it independently. The quality of the fit was measured by minimizing the weighted (biased) test function, namely the mean-squared error (MSE) defined by the Levenberg-Marquardt algorithm [29]. It was observed that introducing interfacial layer between the substrate and the ZnO layers did not improve the mean square error (MSE). All the samples have exhibited a surface roughness layer modeled by Bruggeman effective medium approximation (EMA) containing void and ZnO material. The roughness layer thickness and void percentage were normally fitted along with the ZnO layer while fixing the parameters of the model at the values for the best fit. The results to the fit and other experimental data are listed in Table 1. The difference between measured and calculated film thicknesses is less than 5% with a minimum MSE.

The optical constants (n and k) were then extracted at every experimental wavelength (or photon energy) by means of point-by-point fit. Despite the fact that, the measurements and analyses were carried out between 1.2 to 4.2 eV, as in Figure 1, the curves for the refractive index n as a function of applied power are shown in Figure 3 for the spectral range of our interest (around the band edge) between 2.2 and 4.2 eV. The Sellmeier's model parameters for n are found to be; $A_n = 1.9821$, $B_n = 1.575 \times 10^6$, $C_n = 1 \times 10^8$, $D_n = 1.5835$ and $E_n = 2576.5$ compared to the first-order values obtained in reference [1] as; $A_n = 2.0065$, $B_n = 1.5748 \times 10^6$, $C_n = 1 \times 10^8$, $D_n = 1.5868$ and $E_n = 2606.3$. The two sets of parameters are very comparable. Two peak features at photon

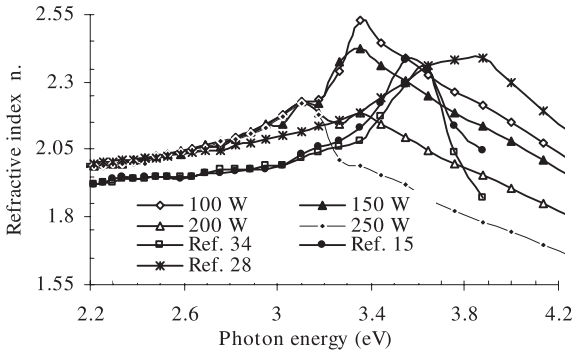

Fig. 3. Refractive index curves for sputtered ZnO films at different applied powers compared with the results in the references [15,28,34].

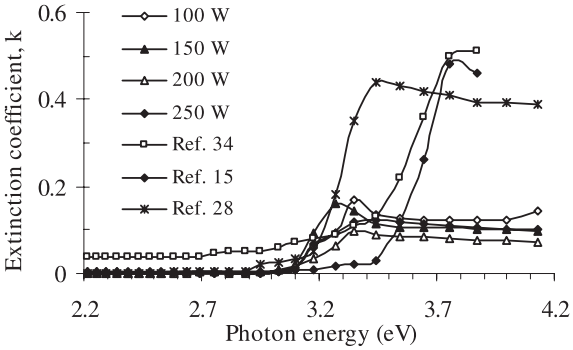

Fig. 4. Extinction coefficient curves for sputtered ZnO films at different applied powers compared with the results in references [15,28,34].

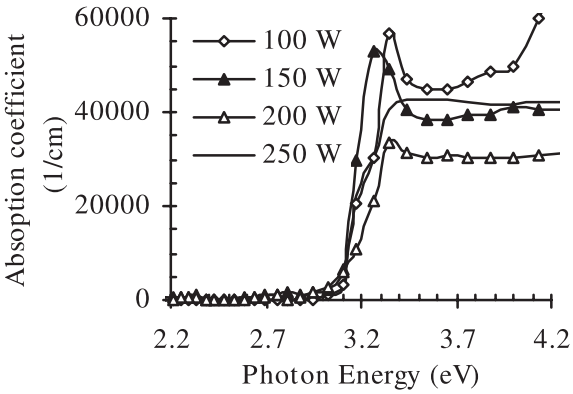

Fig. 5. Absorption coefficient for ZnO films as a function of applied dc power.

energies 3.10 and 3.35 eV are observed in the curves of the refractive indices at all powers (100 to 250 Watts). The shape of the first small peak occurred at energy of 3.1 eV is similar for all studied samples. The second peak is more noticeable for the samples deposited at 100 and 150 Watts applied powers. On the other hand, the curves for the samples deposited at 200 and 250 Watts indicate a rather less intensity peaks at photon energy of 3.35 eV with a downward inclined trend.

The reduction in the second peak intensities is pronounced in such a way that the second peak of the sample deposited at 250 Watts is about to vanish. These features are compared to the values obtained by Jellison and Boatner [22] at 3.114 eV and 3.340 eV photon energies, respectively and attributed to the two discrete excitons associated with a three dimensional critical point in the joint density of states related to the one-electron band structure. The results obtained by Memrazadeh [15] and Matz [34], as seen in Figure 3 are almost comparable to each other below the band edge and have the smaller peak at the same photon energy (3.1 eV) as in our results although appeared at lower refractive index ($n = 1.95$). The second peak in the two curves was found at two different positions, namely 3.55 eV and 3.60 eV, respectively. The refractive index curve obtained by Rebien [28] agrees well with all the curves of our samples in the range way below the band edge. Furthermore, the curve has only one peak at around 3.8 eV with rather higher values on refractive index in most of the spectrum compared to the other references. It can also be seen that, the refractive index curve trend for the sample studied at 250 Watts is different from the corresponding curve trends for the other samples deposited at lower powers. It looks that lower dc power, as long as it is less than or equal to 200 Watts, produces ZnO thin films with features similar to those available in the recent experimental studies.

The curves for the extinction coefficients evaluated as a function of photon energy for different applied dc powers are shown in Figure 4. Cauchy-like parameters were found to be, $F_k = 0.000178$, $G_k = 73271$ and $H_k = 3378.7$. To the best of our knowledge, no numerical values are given in the literature to compare them with our obtained parameters. However, qualitative eye-ball for the line-shape comparison with the extinction coefficient curves in reference [1] gives very good agreement. It is seen that ZnO material given in the three references (Refs. [15,28] and [34]) absorb much more than the films produced in our process. In fact this could be attributed to the polycrystalline microstructural nature of our material compared to the single crystalline ZnO except for reference [15]. The quality of the films depends on the type of the deposition process.

The absorption coefficient curves for the samples, as can be seen in Figure 5, were calculated from the extinction coefficients according to the formula ($\alpha = 4\pi k/\lambda$) [24]. The curves for the samples deposited at 100 and 200 Watts highly agree with experimental and calculated results obtained by Yoshikawa and Adachi [24]. Our samples exhibit strong discrete-exciton peaks at photon energy of 3.35 eV that is similar to their results. However, our samples possess smaller absorption coefficients (5.5×10^4 and 3.5×10^4 cm^{-1}, respectively) compared to the corresponding 2×10^5 cm^{-1} in their work.

On the other hand, the film deposited at 150 Watt possesses similar curve trend but with the discrete-exciton peak found at 3.26 eV and 4×10^4 cm^{-1} absorption coefficient, respectively. The sample deposited at 250 Watt has different curve trend compared to the others. The exciton peak is almost not noticeable. The absorption coefficient

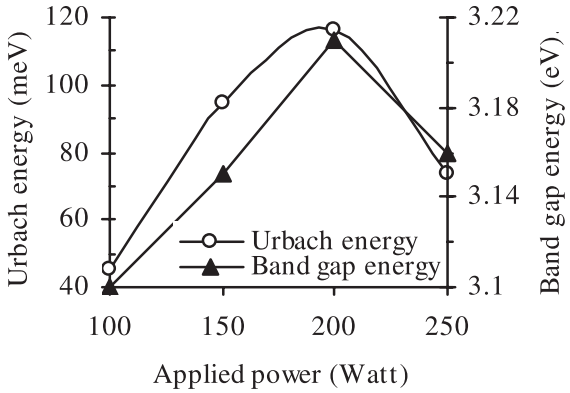

Fig. 6. Urbach's and band gap energies for ZnO films as a function of dc power.

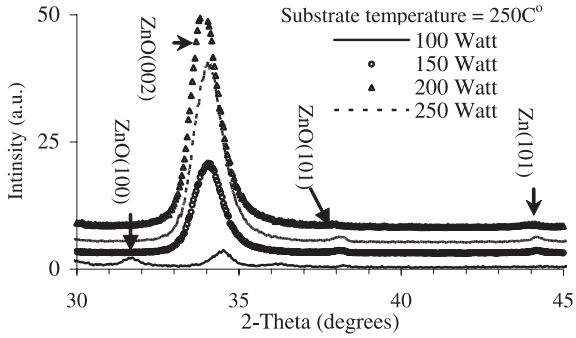

Fig. 7. X-ray diffractions for the sputter deposited ZnO films on Si substrates at different applied powers.

stabilizes at around 4.2×10^4 cm^{-1} for all the spectra over the band edge. In fact, this observation confirms similar observation on the refractive index behavior seen in Figure 4. The optical direct band gaps are evaluated according to the general formula, $(\alpha h\nu)^2 = B(h\nu - E_g)$. Where, B is constant, $h\nu$ is the photon energy and E_g is the optical direct band gap obtained by extrapolating the linear part of the relation above the direct band edge to the zero absorption coefficient. The results are shown in Figure 6.

It is seen that the band gap increases by increasing the applied dc power until it reaches the maximum value (3.21 eV) at 200 Watt. When the applied power is increased to 250 Watts, the band gap decreased to 3.16 eV. This may be attributed to either deposition scenario: (1) by applying low dc power (100 to 200 Watts) to the sputtering gun, argon ions sputter-off zinc atoms from the zinc target that are either reacted with oxygen and deposited as whole (ZnO) on the heated substrate or separately deposited on the substrate to form ZnO stoichiometry. However, at higher dc power (250 Watts) huge number of zinc atoms are sputtered-off the zinc target at high sputtering rate where not all of them are able to react with oxygen neither in their way to the substrate nor at the substrate surface itself; (2) it is believed that the oxygen gas is absorbed by the zinc-target surface and formed a thin ZnO layer. Therefore, applying low dc power (100 to 200 Watts) will sputter ZnO stoichiometry from the top the zinc target which is then deposited in whole on the substrate. Increasing the dc power to higher value (250 Watt) will allow the argon ions to knock deeper into the zinc target through the ZnO layer, or even after removing it, and hence, an excess of pure zinc atoms are sputtered out of the target-skin which will ultimately reach the substrate surface without probably combining with oxygen. In either scenario, it is expected to have an excess of zinc material at higher dc power and this means that isolated zinc atoms could be seen in the microstructure of the films. That is what is confirmed by the X-ray diffraction patterns seen in Figure 7. The role of zinc in modeling the optical properties of ZnO films are expected to play comparative role of Mg in ZnO obtained by Teng et al. [30] which has used the first-order Sellmeier's dispersion relation for a model dielectric function to evaluate the refractive index of MgZnO.

An exponential absorption tail is observed for all films. The Urbach's energies (E_o) are extracted from the steepness of the absorption coefficient tail near the band edge using the formula [28,35]: $1/E_o = d(\mathrm{Ln}\alpha)/d(h\nu)$. The Urbach's energy ($E_o$) related to the applied dc power (P) is shown in Figure 6. The curve is best fitted to the third power polynomial function: $E_o = 5.5 - 0.74\,P + 0.016\,P^2 - 4.84 \times 10^{-5}\,P^3$. Similar curve trend could also be seen by plotting the deposition rate (DR) as a function of applied power (P) as seen in Table 1. In fact, the deposition rate is best fitted to the third power polynomial function as: $\mathrm{DR} = -0.83 + 0.01633\,P - 6 \times 10^{-5}\,P^2 + 6.67\,P^3$. This analogy leads to the conclusion implying that the Urbach's energy (E_o) is directly related to the atomic structural disorder and/or the localized defects in the band associated with the deposition rate consequences. Urbach's energy E_o changes between 44.88 meV and 116.62 meV as the applied power changes according to the relation shown in Figure 6. This range of the values agrees very well with most of the result that we know given almost up to date [36]. In fact exciton-phonon coupling is expected to associate with the light-material interaction of the polycrystalline films performed in our process due to the fact that all films were deposited at 250 °C substrate temperature.

3.2 Microstructure by X-ray diffraction

The X-ray diffraction pattern for ZnO films deposited in our technique have shown a preferred (002) orientation as the applied dc power increases from 100 to 200 Watts (see Fig. 7). If the first scenario of sputter-deposition process discussed above (Sect. 3.1) is the dominant one, then it is believed that applying 100 Watts dc power is not high to sputter enough zinc atoms from the zinc target under the given experimental conditions.

Therefore, no enough zinc atoms are liberated in the gaseous phase to react with the available oxygen ions in order to form oriented ZnO stoichiometry at the substrate surface. However, if an initial thin ZnO layer is formed on the target surface as expected by the second scenario discussed in the same section, then, based on the fact that the

sputtering yield of ZnO is less than that of zinc, 100 Watts is a low power to sputter ZnO rather than what is supposed to be zinc. Moreover, since the power used in our process is a dc rather than rf (which is usually used for ceramic or dielectric material to discharge the target surface every half cycle of its time period), it is expected to have charge accumulation on the top of the target surface, and hence, an ultimate reduction to the sputtering efficiency. This phenomenon is crucial to the optical and structural properties of the films. By rather increasing the dc power to 150 Watts, more (002) ZnO material is deposited and very small sign of (101) ZnO orientation is formed. The best dc power needed to form high quality (002) material is 200 Watts. As the power is increased to 250 Watts, the (002) peak is reduced in favor of forming weak ZnO(101) and Zn(101) peaks as seen in Figure 7. It is believed therefore, that high sputtering power produces excess of zinc atoms that are deposited on the surface of the substrate before they are compensated in the ZnO stoichiometry. In fact, this confirms the prediction of different optical behavior at 250 Watt sputtering power (see Figs. 3–6). This absorption behavior is believed to occur due to the formation of an interband transitions caused by the uncompensated metallic zinc atoms. These atoms were embedded in the films as either an incoming atoms reached the substrate without reacting with oxygen in the gaseous phase, or as atoms left in the films after oxygen atoms are liberated due to the thermal activation caused by the substrate temperature (250 °C).

4 Conclusions

This is the first attempt to study the optical properties of unbalanced magnetron sputter deposited ceramic ZnO films on Si(100) from metallic zinc target, using argon and reactive oxygen, relative to the dc applied power. The optical constants were extracted by VASE of ψ and Δ by a second-order Sellmeier equation for refractive index and Cauchy-like dispersion model for the extinction coefficient. The Urach's energies and optical band gaps were related to the deposition rate and found to correlate with each others while varying with applied power. The X-ray diffraction patterns were reported and related to the optical behavior.

The Authors would like to acknowledge Prof. N. Ianno at the Center for Microelectronics and Optical Materials Research and the Department of Electrical Engineering at the University of Nebraska-Lincoln, the United States of America, for his support in films deposition and Prof. N. Ayoub, the Dean of School of Natural Sciences at German-Jordanian University in Amman – Jordan for his valuable advices.

References

1. X. Sun, H. Kwok, J. Appl. Phys. **86**(1), 408 (1999)
2. S. Lee, Y. Im, Y. Hahn, Korean J. Chem. Eng. **22**(2), 334 (2005)
3. V. Karpina et al., Crys. Res. Technol. **39**(11), 980 (2004)
4. B. Lin, Z. Fu, Y. Zia, Appl. Phys. Lett. **79**, 943 (2001)
5. S. Jeong, I. Kim, S. Kim, J. Kim, B. Lee, J. Cryst. Growth **264**, 110 (2004)
6. S. Jeong, I. Kim, J. Kim, B. Lee, J. Cryst. Growth **264**, 327 (2004)
7. S. Roy, S. Basu, Bull. Mater. Sci. **25**(6), 513 (2002)
8. S. Pittal, L. McConville, N. Ianno, P. Snyder, Mat. Res. Soc. Symp. Proc. **236**, 423 (1992)
9. T. Shioski, T. Yamamoto, M. Yagi, A. Kawabata, Appl. Phys. Lett. **39**, 399 (1981)
10. S. Demian, J. Mater. Sci. Mater. Elec. **5**, 360 (1994)
11. Z. Jiwei, Z. Kianging, Y. Xi, Ceramics International **26**, 883 (2000)
12. T. Subramanyam, B. Naidu, S. Uthanna, Crystal Research Technology **34**(8), 981 (2000)
13. T. Subramanyam, B. Naidu, S. Uthanna, Crystal Research Technology **35**(10), 1193 (2000)
14. X. Meng, W. Zhen, J. Guo, X. Fan, Appl. Phys. A **70**, 421 (2000)
15. K. Memarzadeh, J. Woollam, A. Belkind, *SPIE* **823**, *Optical Materials Technology for Energy Efficiency and Solar Energy Conversion* VI, 54 (1987)
16. T. Yamamota, T. Shiosaki, A. Kawabata, J. Appli. Phys. **51**, 3113 (1980)
17. X. Meng, W. Zhen, J. Guo, X. Fan, Appl. Phys. A **70**, 421 (2000)
18. J. Woollam, P. Snyder, *Review of Progress in Quantitative Nondestructive Evaluation,* 10 B, edited by D.O. Thompson, D.E. Chimenti (Plenum Press, NY, 1991), p. 22185
19. R. Azzam, N. Bashara, *Ellipsometry and Polarized Light* (North Holland Press, Amsterdam and NY, 1977)
20. K. Postava, H. Sueki, M. Aoyama, T. Yamaguchi, Ch. Ino, Y. Igasaki, M. Horie, J. Appl. Phys. **87**, 7820 (2000)
21. M. Erman, J. Theeten, P. Chambon, S. Kelso, D. Aspens, J. Appl. Phys. **56**(10), 2664 (1984)
22. G. Jellison Jr, L. Boatner, Phys. Rev. B **58**, 3586 (1998)
23. T. Holden, P. Ram, H. Pollak, J. Freeouf, B. Yang, M. Tamargo, Phys. Rev. B **56**, 4037 (1997)
24. H. Yoshikawa, S. Adachi, Jpn Appl. Phys. I **36**, 6237 (1997)
25. W. Bond, J. Appl. Phys. **36**, 1674 (1965)
26. E. Heltemes, H. Swinney, J. Appl. Phys. **38**, 2387 (1967)
27. P. Yeh, *Optical waves in layered media* (Wiley, NY, 1988)
28. M. Rebien, M. Henrion, M. Bar, Ch.H. Fishcher, Appl. Phys. Lett. **80**, 3518 (2002)
29. C. Herzinger, P. Snyder, B. Johs, J. Woollam, J. Appl. Phys. **77**(4), 1715 (1995)
30. C. Teng, J. Muth, U. Ozgur, M. Bergmann, H. Everitt, A. Sharama, C. Jin, J. Narayan, Appl. Phys. Lett. **76**, 979 (2000)
31. J. Muth, R. Kolbas, A. Sharma, S. Oktyabrsky, J. Narayan, J. Appl. Phys. **85**, 7884 (1999)
32. L. Bai, Ch. Xu, P. Schunemann, K. Nagashio, R. Feigelson, N. Giles, J. Phys. Condens. Matter **17**, 549 (2005)
33. D. Aspnes, A. Studna, Phys. Rev. B **27**, 7466 (1983); D. Aspnes, A. Studna, in *Handbook of optical constants of solids*, edited by E.D. Palik I (Academic, Orlando, FL, 1985), Chap. 5
34. R. Matz, H. Luth, Appl. Phys. **18**, 123 (1979); T. Datta, J. Woollam, Phys. Rev. B **40**, 5956 (1984)
35. M. Kurik, Phys. Status Solidi A **8**, 9 (1971)
36. N. Aghamalan, E. Kafadaryan, R. Hovsepyan, S. Petrosyan, Semicond Sci. Technol. **20**, 80 (2005)